Martensite formation in 9 Cr-1 Mo steel weld metal and its effect on creep behavior

M. L. Santella[*], R. W. Swindeman[*], R. W. Reed[*], and J. M. Tanzosh[#]
[*]Oak Ridge National Laboratory, Oak Ridge, Tennessee 37831
[#]Babcock & Wilcox Company, Barberton, Ohio 44203

Abstract

Maximizing the efficiency of power boilers generally requires operation at the highest possible temperatures and steam pressures. In turn, these more aggressive operating conditions require the use of higher strength materials than were typically used for the construction of power plants. This situation has increased the interest in issues related to the processing and fabrication of alloys such as 9Cr-1Mo-V (P91) steels. The P91 steels are high strength alloys that normally transform completely to martensite during air cooling. This means that the specification of preheating and post weld heat treating conditions is an important concern. One important issue is specification of maximum tempering temperatures which are limited by the lower critical temperature for the ferrite-to-austenite phase transformation, A_1. A similar issue is related to the handling of weldments between the completion of welding and post weld heat treatment. Computational thermodynamics was used to analyze the effects of major alloying elements on A_1. The analysis verified that (Mn+Ni) concentration has the strongest influence on A_1 of P91 steels, and an expression relating A_1 to (Mn+Ni) was developed. Experimental measurements indicated that the predicted A_1 may be underestimated at higher (Mn+Ni) concentrations. Measurements of specimen dilations during controlled thermal cycles were used to follow the martensite transformation in a P91 base metal and a weld deposit. For identical thermal cycles, the base metal transformed completely to martensite after normalizing, but the weld deposit did not. The effect of this difference in transformation behavior was that austenite was retained in the weld deposit after tempering. The retained austenite transformed to martensite upon cooling from the tempering temperature, resulting in small amounts of untempered martensite in fully heat treated weld deposit. Creep testing at 600°C and stresses of 120 MPa and 186 MPa showed that weld deposit specimens with untempered martensite had low creep rates and relatively long rupture lives.

Introduction

In the early 1980's, tubing of 9Cr-1Mo-V steel (P91) began being introduced into the superheaters of power boilers as a replacement for 300 series austenitic stainless steels [1]. The P91 steels have several advantages compared to the austenitic alloys. The thermal expansion coefficient of P91 is lower than those of austenitic stainless steels and its thermal conductivity is higher. These properties improve the resistance of P91 to thermally-induced stresses and they provide a better match of properties with the lower alloy steels used throughout other components of the boilers. The higher thermal conductivity also improves heat transfer through tubing walls into cooling water. Also, P91 steels have relatively good oxidation resistance at intermediate temperatures and can exhibit high strengths up to about 600°C [2]. Lastly, for any given product form, P91 steel will generally cost less than austenitic alloys so the economic incentive to use P91 can be significant depending on the specific application.

Because P91 steel is a high strength alloy that normally transforms completely to martensite during air cooling [3], the specification of preheat and post weld heat treating (PWHT) conditions is an important concern. One important issue is specification of the maximum temperature for PWHT. The ASME Codes, such as Section VIII, require a minimum PWHT temperature of 704°C (1300°F). However, P91

is relatively resistant to tempering, and higher PWHT temperatures are generally needed to reduce hardness in weld heat-affected zones and to develop the necessary toughness in weld deposits [4]. When increasing PWHT temperatures, care must also be taken to avoid exceeding the lower critical temperature for the ferrite-to-austenite transformation, A_1. If the A_1 is exceeded, then austenite will reform in the microstructure. This 'fresh' austenite will then partially or completely transform to martensite on cooling from the PWHT temperature, and it will result in untempered martensite in the final microstructure. Another related issue is the handling of weldments between completion of welding and PWHT. Weldments that are cooled to room temperature prior to PWHT will transform more completely to martensite than weldments that are maintained at or above minimum preheat temperature prior to PWHT. Consequently, weldments that are cooled to room temperature are less likely to contain untempered martensite after PWHT. However, maintaining preheat temperature prior to PWHT is essential for minimizing the probability of hydrogen cracking in weld heat-affected zones. In addition, it makes more efficient use of energy resources, and it may be desirable for practical reasons depending on the welded component size and the available facilities for material handling and heat treating.

This paper describes the initial analysis and testing of a submerged arc weldment made in 2-in-thick P91 plate. The influence of chemical composition on the A_1 was analyzed using computational thermodynamics (ThermoCalc™ software). An expression relating A_1 to (Mn+Ni) was developed and compared with some experimental results. The transformation behavior after normalizing and tempering of the weld deposit and a P91 base metal was determined from specimen dilations measured during controlled heating and cooling using a Gleeble™ thermomechanical simulator. Creep testing of weld deposit specimens was done in air at 600°C (1112°F) at stresses of 120 MPa (17.4 ksi) and 186 MPa (27 ksi).

Materials and Experimental Details

The chemical compositions of the alloys used for this work are given in Table 1. The submerged arc weld was made using Thermanit MTS3 welding filler metal (AWS A5.28, ER90S-B9) and Marathon 543 flux, both products of Böhler Thyssen. The 2-in-thick plate used for the weldment was produced by Bethlehem Lukens Plate and is identified as BLP9Cr in Table 1. The plates were prepared for welding with a single-vee groove using a 60° included angle. A macrophotograph of the weldment is shown in Fig. 1. A total of 44 weld beads was used to complete the weldment. The weldment was given a PWHT of 8 hours at 774°C (1425°F) before being supplied for testing and analysis. Specimens from normalized and tempered plate identified as heat 30383 were used to establish baseline transformation behavior for P91 plate. This also permitted more of the weldment to be committed to mechanical test specimens.

Table 1. Alloy chemical compositions

	Analyzed composition, wt%									
ID/heat	C	Mn	Si	Cr	Mo	Ni	Nb	V	N	Al
Weld	0.099	0.61	0.17	9.33	0.97	0.80	0.043	0.23	0.051	0.022
BLP9Cr	0.10	0.41	0.33	8.61	0.90	0.14	0.067	0.21	0.056	0.028
30383	0.083	0.46	0.41	8.46	1.02	0.09	0.072	0.198	0.051	0.002

A Gleeble™ 3500 thermomechanical simulator was used to determine the A_{C1} temperatures by heating specimens from below to above the expected A_1. At relatively slow heating rates the A_{C1} provides a reasonable approximation of the A_1. The M_S temperatures where martensite starts to form during cooling were also determined. The Gleeble heats specimens resistively, and it uses the feedback from a thermocouple attached to each specimen to control temperature. This arrangement permits very rapid

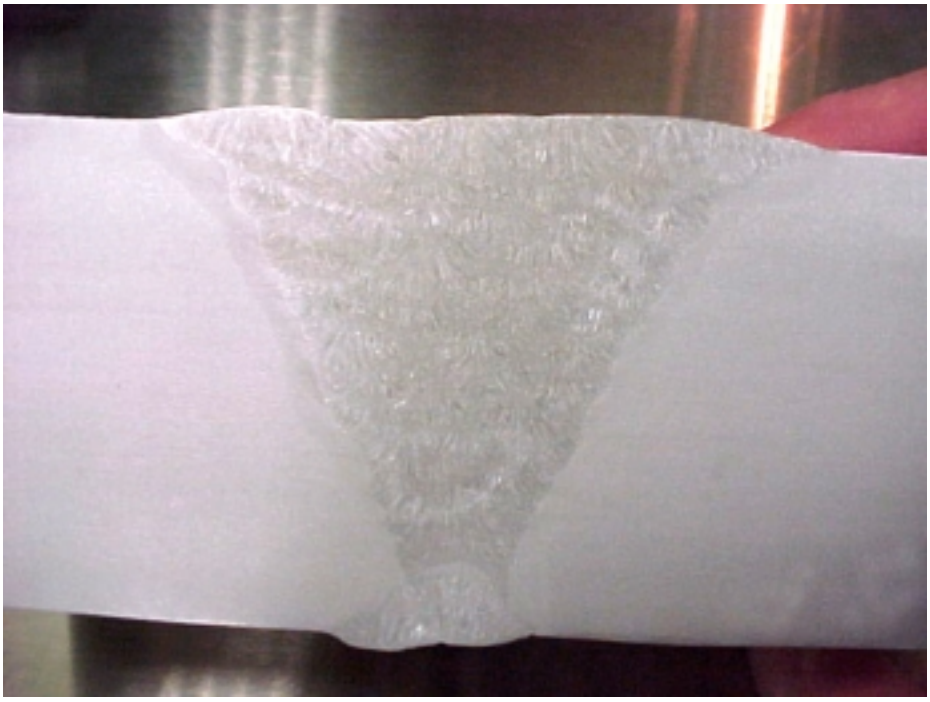

Fig. 1. *Macrophotograph showing a cross-section view of the submerged arc weldment used for testing and analysis. The P91 plate was 2 in thick.*

heating and cooling rates, and complex thermal cycles. The Gleeble specimens used for this study were 6.35 mm (0.25 in) diameter x 108 mm (4.25 in) long rods. In the weld deposit, the rods were cut transverse to the welding direction from near the weld surface. The width of the weld at this location was about 45 mm (1.75 in). This insured that the section of the specimen that was actually heated was entirely within the weld deposit. The dilation of the specimens during heating and cooling was measured with an LVDT strain gauge configured to detect changes in specimen diameter. The strain gauge was attached at the same location along the specimen length as the thermocouple. The specimens were heated either in vacuum or argon atmosphere to minimize oxidation during testing. Transformation temperatures were determined by curve fitting procedures at points of significant discontinuity on dilation-versus-temperature data plots.

For mechanical testing, bar specimens with either 6.35 mm (0.25 in) or 9.53 mm (0.375 in) diameters were machined parallel to the welding direction from the weld deposit. These specimens were tested in the as-received, PWHT condition. Other 6.35-mm-diameter specimens were machined transverse to the welding direction near the top of the weld deposit, and they had reduced sections of 25.4-mm-long that were entirely in the weld metal. The transverse specimens were machined from 12.5-mm-thick slices of the original welded plate. These slices were given the following heat treatments:

1. Normalize for 15 min at 1040°C (1904°F)
2. Air-cool either to room temperature or to 200°C (392°F)
3. Temper either for 30 min at 740°C (1364°F) or for 1 h at 780°C (1436°F)
4. Air-cool to room temperature.

The creep-rupture testing was performed in 12/1 lever-arm creep frames following ASTM 139. Testing was done in air at 600°C using stress levels of 120 MPa (17.4 ksi) and 186 MPa (27 ksi). Extensometers were attached to the specimen shoulders to measure the extension with time.

Results

Effect of P91 composition on A_1: The effects of the major alloying elements on the A_1 of P91 steel were evaluated using ThermoCalc™ software. ThermoCalc™ uses theoretical thermodynamic models and databases of measured thermochemical properties to calculate phase equilibria in multiphase, multicomponent systems. The computational procedures are based on minimization of Gibbs energy [5]. The approach used for predicting the A_1 of P91 alloys was based on using the chemical composition range specified by ASTM. A reference composition was chosen with elements at or near the midrange values. The reference composition and specified composition ranges are shown in Table 2. In each case the balance of the alloy is Fe. Evaluation of the individual effects of C, Si, Cr, Mo, Nb, V and N involved using the reference composition and varying only the element of interest between the minimum and maximum values shown in Table 2.

Table 2. *P91 compositions used for A_1 predictions*

	Wt% of element in P91								
Condition	C	Mn	Si	Cr	Mo	Ni	Nb	V	N
Minimum	0.08	0.30	0.20	8.0	0.85	---	0.06	0.18	0.03
Reference	0.10	0.45	0.35	9.0	1.0	0.20	0.08	0.22	0.05
Maximum	0.12	0.60	0.50	9.5	1.05	0.40	0.10	0.25	0.07

The predicted A_1 for the reference composition was 822°C (1512°F). The variation of A_1 for the ranges of C, Cr, Mo, and N shown in Table 2, are presented in Table 3. The effect of Si on A_1 was negligible. The effects of Nb and V were evaluated in combination. At their combined minimum specified concentrations (0.06 Nb + 0.18 V) the predicted A_1 was 818°C (1504°F). At their combined maximum specified concentrations (0.10 Nb + 0.25 V) the predicted A_1 was 823°C (1513°F).

Table 3. *Predicted variations of A_1 for C, Cr, Mo, and N based on reference P91 composition*

	Wt %		A_1 (°C/°F) at	
Element	minimum	maximum	Minimum	maximum
C	0.08	0.12	824/1515	820/1508
Cr	8.0	9.5	817/1503	824/1515
Mo	0.85	1.05	818/1504	824/1515
N	0.03	0.07	825/1517	812/1494

The variation of A_1 with (Mn+Ni) was evaluated in more detail. In this case, Mn concentration was successively set to levels of 0, 0.3, 0.6, 0.75, 1.0, and 1.2 wt%. At each Mn concentration, the Ni concentration was set to levels of 0, 0.1, 0.2, 0.4, 0.6, 0.8, 1.0, and 1.2 wt%. The Mn and Ni levels beyond the limits shown in Table 2 where used because these higher concentrations appear in specifications for welding electrode compositions. The A_1 was calculated for each (Mn+Ni) combination. The A_1 values representing these 48 equilibrium calculations were then combined into a single plot and a three-term polynomial function was fit through the data. This plot is shown as Fig. 2. The best fit line through the data gives the following expression for the variation of A_1 with (Mn+Ni):

$$A_1,°C = 854.5 \pm 0.6 - 43.9 \pm 1 \times (Mn+Ni) - 9 \pm 0.4 \times (Mn+Ni)^2$$

$$A_1,°F = 1570 \pm 1.0 - 79.0 \pm 1.8 \times (Mn+Ni) - 16.1 \pm 0.7 (Mn+Ni)^2$$

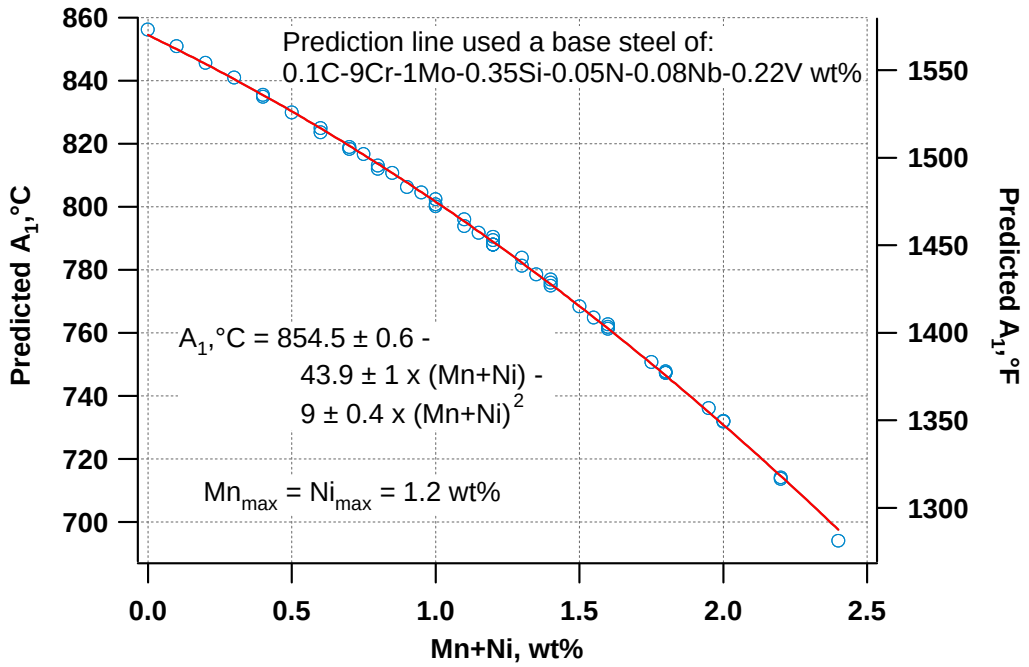

Fig. 2. *Prediction based on equilibrium thermodynamics of the variation of A_1 with (Mn+Ni) concentration in P91 steel.*

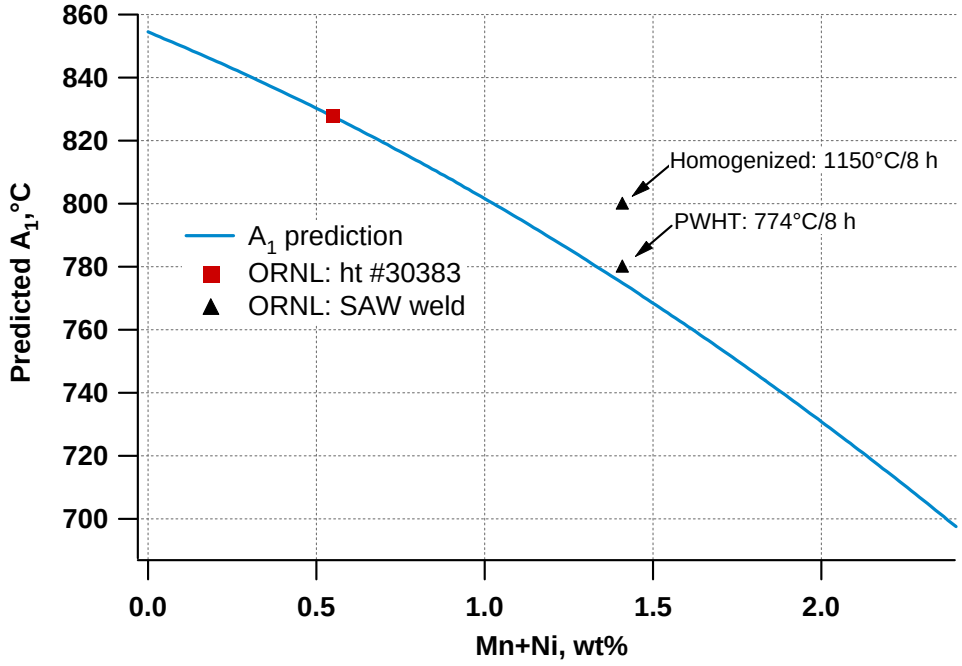

Fig. 3. *Comparison of predicted A_1 and experimentally measured A_{C1} temperatures.*

This equilibrium prediction is based on the reference composition shown in Table 2 for the elements other than Mn and Ni. Variations in the other major alloying elements will affect the A_1 as shown in Table 3, but their influence is secondary to that of Mn and Ni concentrations. The A_{C1}'s were measured for alloy 30383 and the weld deposit. Three heating rates were used for alloy 30383: 2000°C/min, 20°C/min and 2°C/min. The respective A_{C1} temperatures were 881°C, 845°C and 828°C. This confirms that the detected A_1 depends on the heating rate. The submerged arc weld metal was evaluated only at the lowest heating rate. One weld metal specimen was tested in the PWHT condition and one was tested after an additional homogenization heat treatment of 8 hours at 1150°C. The respective A_{C1} temperatures for the weld deposit were 780°C and 800°C. The measured A_{C1}'s are compared to the A_1 prediction in Fig. 3. Agreement between prediction and measurement for alloy 30383 was excellent. The homogenization heat treatment increased the A_1 of the weld deposit, causing it to be under-predicted by the thermodynamic analysis.

Martensite transformation behavior: The transformation behavior of the submerged arc weld deposit and the alloy 30383 base metal was determined for two similar thermal cycles consisting of:

1. Normalizing for 2 min at 1040°C (1904°F)
2. Cooling to either room temperature or 200°C (392°F)
3. Tempering for 15 min at 740°C (1364°F)
4. Cooling to room temperature at 6°C/min.

The specimen dilation results are shown in Figs. 4 and 5 for alloy 30383, and in Figs. 6 and 7 for the weld deposit. Transformation of the base metal alloy 30383 was the same for cooling to either room temperature or 200°C after normalizing. The martensite start temperature, M_S, for both cases was 393-395°C (739-743°F). In both cases, the martensite reaction in alloy 30383 appeared to be completed prior to the tempering portion of the treatment because no other phase transformation was detected. In contrast, the transformation of the weld deposit was influenced by the temperature to which it was cooled following normalizing. In both cases, a secondary martensite reaction was detected in the weld deposit after tempering. The primary M_S for the weld deposit was 348-350°C (658-662°F). The secondary M_S was near 400°C (752°F). Also, the magnitude of the dilation associated with the secondary martensite reaction was smaller in the specimen that was cooled to room temperature, indicating that this specimen transformed to a higher fraction of martensite during initial cooling from the normalizing temperature. These results show that the weld deposit is likely to contain some untempered martensite after welding and PWHT.

Creep testing: Data from the creep tests of the weld deposit are shown in Fig. 8 for the 120 MPa stress level and in Fig. 9 for the 186 MPa stress level. At both stress levels, the creep rates were highest for the as-received PWHT specimens. The creep rates were lowest for specimens that were normalized, cooled to 200°C, and then tempered. Increasing the stress from 120 MPa to 186 MPa also significantly increased the creep rates of all three specimen types. The normalizing and tempering treatments subsequent to PWHT significantly extended the rupture life of the weld deposit at 186 MPa.

Discussion

It should be emphasized that the thermodynamic calculations on which the A_1 prediction was based describe sets of equilibrium conditions. In addition to the ferrite-austenite equilibrium, it considers that the equilibrium fractions of second phases such as carbides, nitrides, or carbonitrides are precipitated, and that the alloy is otherwise chemically homogeneous. The calculation of a small decrease in A_1 with increasing C concentration in P91 agrees with published C-Cr-Fe phase diagrams [6,7]. The equilibrium calculations further indicate that Cr, Mo, Si, Nb, and V have only small effects on A_1, resulting in individual shifts of less than 10°C. The A_1 is increased by Cr, Mo, and (Nb+V). Increasing N from

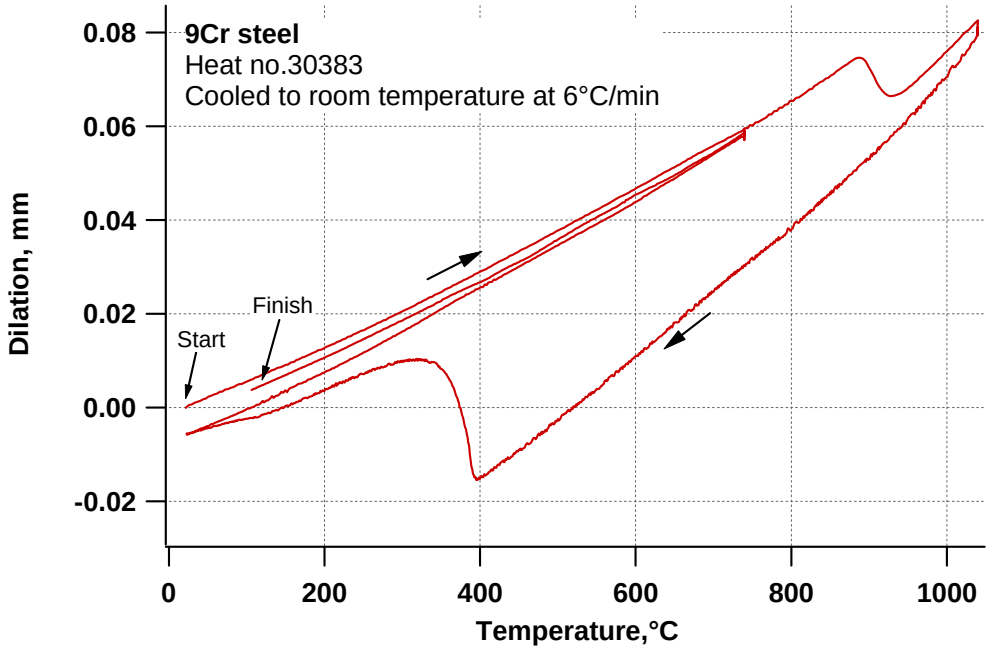

Fig. 4. *Dilation response of base metal alloy 30383 specimen cooled to room temperature after normalizing.*

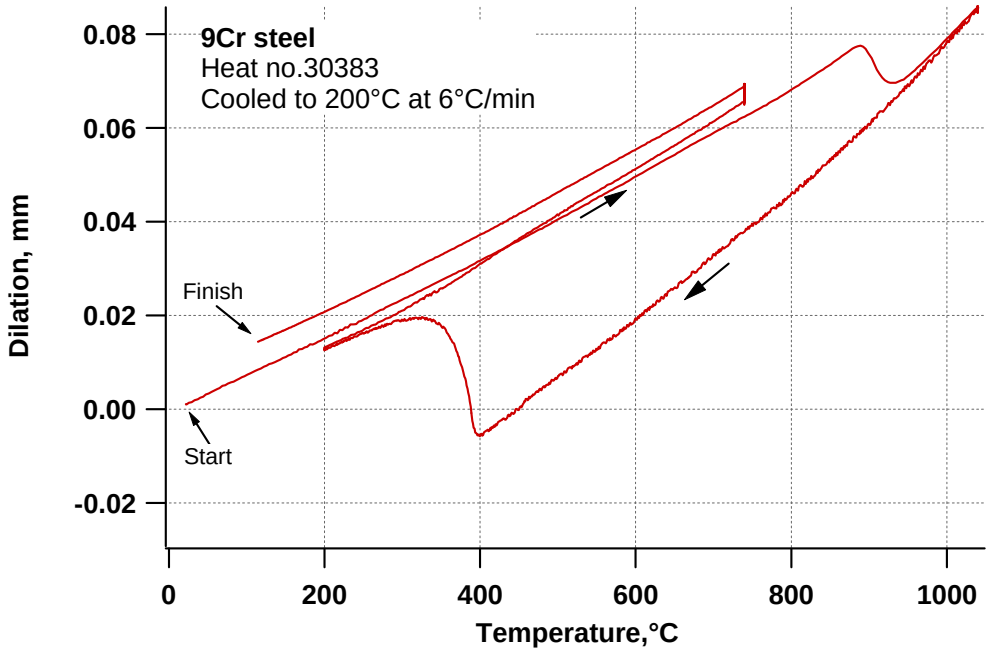

Fig. 5. *Dilation response of base metal alloy 30383 specimen cooled to 200°C after normalizing.*

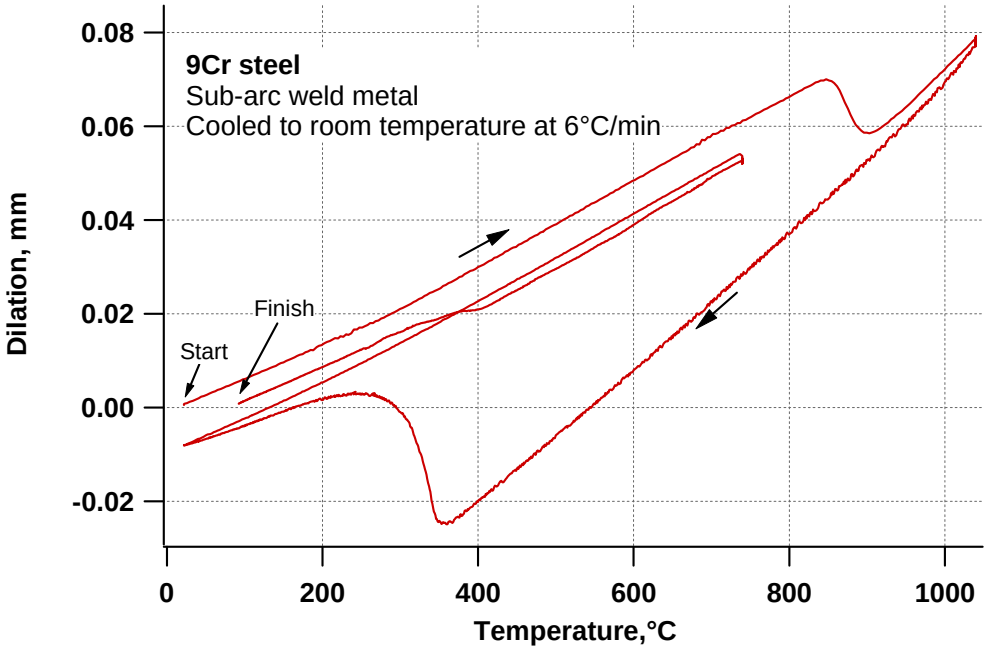

Fig. 6. *Dilation response of submerged arc weld deposit specimen cooled to room temperature after normalizing.*

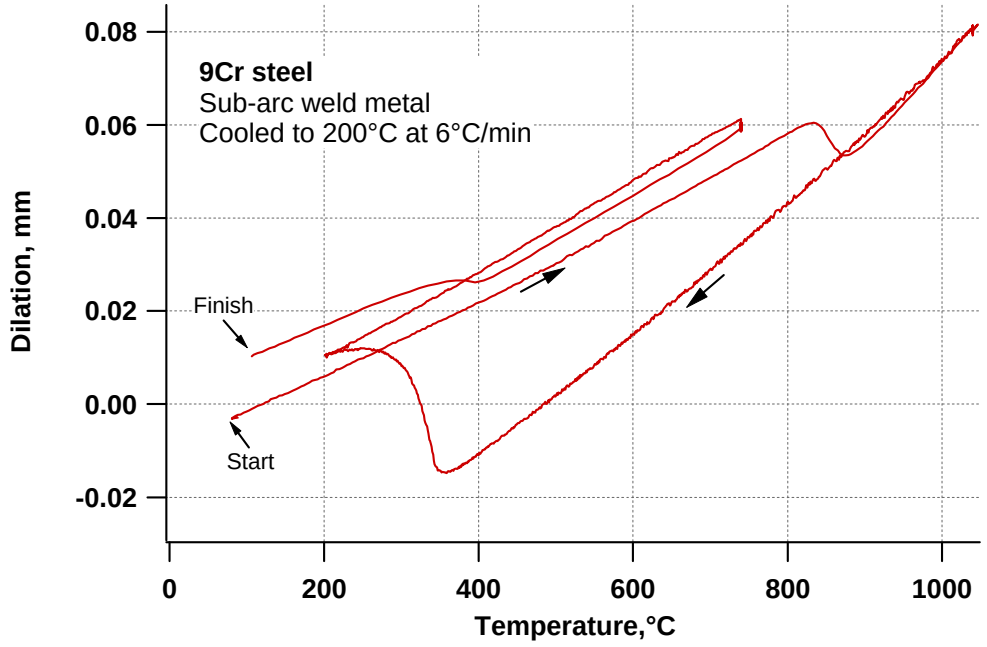

Fig. 7. *Dilation response of submerged arc weld deposit specimen cooled to 200°C after normalizing.*

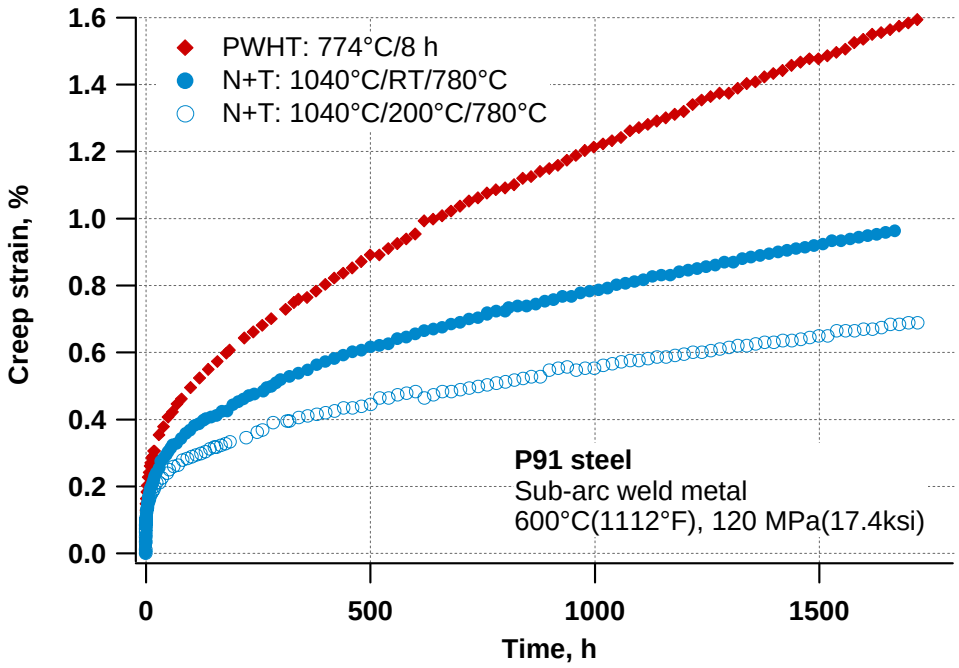

Fig. 8. *Plot of creep strain with time for weld deposit specimens tested at 600°C at a stress of 120 MPa.*

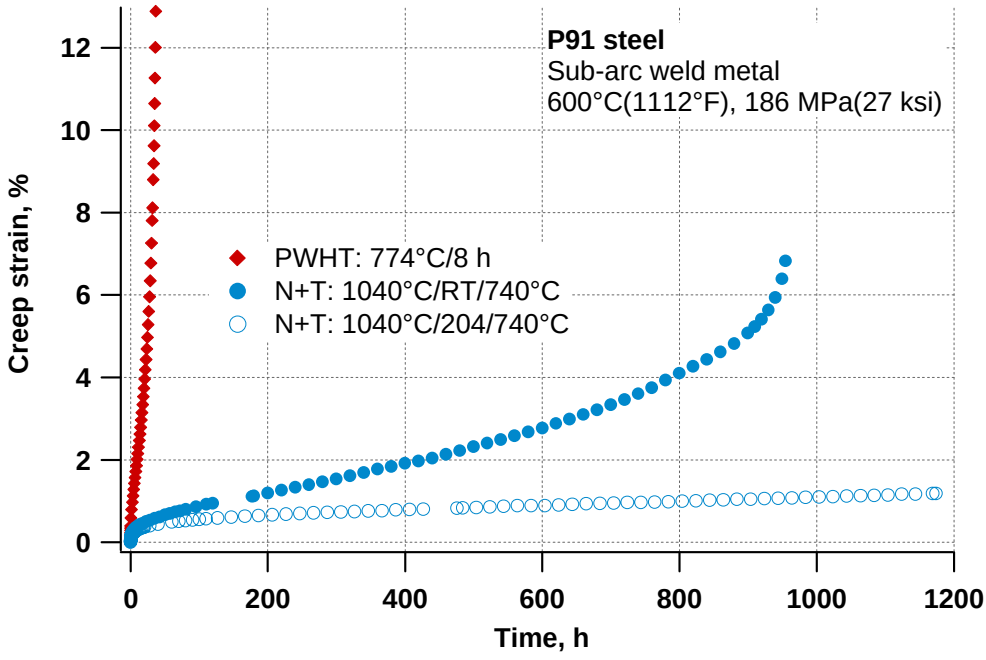

Fig. 9. *Plot of creep strain with time for weld deposit specimens tested at 600°C at a stress of 186 MPa.*

minimum to maximum specified concentration produced a moderate, 13°C, decrease of A_1. The (Mn+Ni) amount had the largest effect on A_1. When neither element was present in the reference P91 composition, the A_1 was predicted to be 856°C (1573°F). At the other extreme condition of having both elements present at 1.2 wt% each, the calculated A_1 was 694°C (1281°F). Overall, the thermodynamic calculations indicate that the ferrite stabilizing (Cr, Mo) elements increase A_1, while the austenite stabilizing elements (C, Mn, Ni, N) decrease A_1.

The increase of measured A_{C1} with heating rate is consistent with the behavior of ferrite-austenite transformations in Fe-C alloys [8]. The variation of A_{C1} with heating rate also affirms the importance of considering this dependence when experimental A_{C1} measurements are evaluated or reported.

A possible explanation of the effect of the homogenization heat treatment on the A_{C1} of the weld deposit specimens stems from consideration of microsegregation. Attempts to identify microsegregation patterns in the weld deposit by electron probe microanalysis were unsuccessful. However, it is expected that microsegregation will occur in the weld deposit, and that it will result in periodic fluctuations of alloying elements throughout the microstructure. Because of their generally low diffusion rates, especially in austenite [9], the compositional fluctuations of substitutional alloying elements such as Cr, Mn, and Ni will be persistent in the microstructure. Tempering treatments are not likely to provide the thermal activation needed to homogenize the distributions of substitutional elements. Areas of the microstructure of the weld deposit where (Mn+Ni) concentrations are elevated should therefore have depressed A_1's (or A_{C1}'s) relative to that of the bulk composition. If the volume which contains elevated (Mn+Ni) is significant, then it will lower the A_{C1} value detected by measuring dilation response. By this same reasoning, homogenizing the (Mn+Ni) concentrations should increase the detected A_{C1}. This general pattern agrees with the experimental data plotted in Fig. 3 for the weld deposit, i.e., the A_{C1} after homogenization heat treatment was 20°C higher than that before homogenization. Because the homogenized specimen should more closely represent equilibrium, these two data points also suggest that the thermodynamic prediction may underestimate A_1 by about 20°C. Other factors can also influence these results. For instance, the homogenized specimen may be supersaturated relative to carbonitride precipitation near A_1. Certainly, further testing, including microstructure analysis, and a larger body of experimental data will be needed to judge the general accuracy of this A_1 prediction.

The M_S temperatures for alloy 30383 and the weld deposit agree well with recently published expressions for the prediction of this transformation start temperature [10]. The predicted and measured M_S's for alloy 30383 are 383°C and 393-395°C; those for the weld deposit are 348°C and 347-350°C. The behavior of alloy 30383 is also consistent with analysis indicating that the temperature below which the martensite transformation is finished, $M_F = M_S$ – (180-200°C) [10]. Based on this expression, the martensite transformation in alloy 30383 should be completed after cooling to about 190-210°C. An M_F in this range is consistent with the dilation measurements shown in Fig. 5. These data show that cooling to 200°C is enough to completely transform to martensite, or at least to a level sufficiently high that further transformation after tempering is undetectable.

The weld deposit behavior is not consistent with the M_F prediction of about 150-170°C. According to the M_F relationship, the martensite transformation in the weld deposit should have been completed upon cooling to room temperature, but not 200°C. The dilation results shown in Figs. 6 and 7 indicate that both normalizing and tempering cycles produced microstructures with retained austenite, some or all of which transformed to martensite at around 400°C upon cooling from the tempering temperature. The higher M_S after tempering indicates that the martensite formed after tempering transformed from austenite having a lower carbon concentration than the original, as-normalized austenite. Both normalizing and tempering cycles produced some untempered martensite in the weld deposit.

The heating and cooling rates used to determine the transformation behavior of the weld deposit do not reproduce exactly those used for normalizing and tempering coupons for preparing creep test specimens. Other variations were used for tempering the creep test specimens. The dilation test specimens were tempered for 15 min at 740°C(1364°F). The creep test coupons were tempered for either 30 min at 740°C or for 1 h at 780°C. Nevertheless, it was expected that the specimens used for creep testing of the weld deposit contained some amount of untempered martensite, and that the amount was greater in the specimens that were only cooled to 200°C prior to tempering. The creep data plotted in Figs. 8 and 9 show that for either tempering condition, lower creep strains developed for cooling to 200°C prior to the tempering treatment. These data suggest that creep rates are lowered in weld deposit microstructures containing small amounts of untempered martensite. It is assumed that the high creep rates experienced by the specimens that were only PWHT are mainly due to the softening associated with their longer tempering time of 8 h. The short rupture life of the PWHT specimen at 186 MPa was also likely due to the more extensive softening caused by the tempering heat treatment.

Summary

Analysis of P91 steel compositions using computational thermodynamics was done to analyze the effects of major alloying elements on A_1. The analysis verified that (Mn+Ni) concentration has the strongest influence on A_1 and the results were used to develop the expression:

$$A_1,°C = 854.5 \pm 0.6 - 43.9 \pm 1 \text{ x } (Mn+Ni) - 9 \pm 0.4 \text{ x } (Mn+Ni)^2$$

$$A_1,°F = 1570 \pm 1.0 - 79.0 \pm 1.8 \text{ x } (Mn+Ni) - 16.1 \pm 0.7 \ (Mn+Ni)^2$$

Experimental measurements indicated that A_1 may be underestimated at higher (Mn+Ni) levels. These measurements also suggest that microsegregation may influence A_{C1} measurements using dilation response during controlled heating.

Measurements of dilation during controlled thermal cycles were used to follow the martensite transformation in a P91 base metal alloy and in a weld deposit that was previously post-weld heat treated at 774°C (1425°F) for 8 h. These measurements showed that a secondary martensite reaction occurred during cooling from the normalizing and tempering treatment. This secondary martensite reaction occurred at a higher temperature, $M_S \approx 400°C$, than the primary martensite transformation, $M_S \approx 350°C$. These observations indicate that some austenite was retained in the weld deposit after normalizing and cooling to either room temperature or 200°C, and after tempering. The amount of retained austensite appeared to be greater for cooling to 200°C. The higher M_S of the secondary reaction indicates that the austenite retained through the full heat treating schedule had a lower carbon concentration than the original, as-normalized austenite.

Creep testing at 600°C at stresses of 120 MPa and 186 MPa indicated that the weld deposit specimens that were normalized, cooled to 200°C, and then tempered had the lowest measured creep rates. Cooling to 200°C resulted in lower creep rates than did cooling to room temperature. The lower creep rates of the weld deposit were attributed to higher amounts of untempered martensite after full heat treatment.

Acknowledgment

This research, done at Oak Ridge National Laboratory, was sponsored by the Office of Fossil Energy, Advanced Research Materials Program, (DOE/FE AA 15 10 10 0) U.S. Department of Energy under Contract DE-AC05-00OR22725 with UT-Battelle, LLC. The encouragement of and helpful discussions

with Bill Newell of Euroweld, Ltd. are greatly appreciated. Technical reviews of the manuscript by S. S. Babu and R. L. Klueh are also appreciated.

References:

1. F. V. Ellis, J. F. Henry, and B. W. Roberts, "Welding, Fabrication, and Service Experience with Modified 9Cr-1Mo Steel," pp. 55-63 in *New Alloys for Pressure Vessels and Piping*, PVP Volume 201, American Society of Mechanical Engineers, NY, 1990.

2. V. K. Sikka, C. T. Ward, and K. C. Thomas, "Modified 9Cr-1Mo Steel – An Improved Alloy for Steam Generator Application," pp. 65-84 in *Ferritic Steels for High-Temperature Applications*, edited by A. K. Khare, American Society for Metals, Metals Park, OH, 1983.

3. T. Wada, *The Continuous Cooling Transformation Diagram and Tempering Response of 9Cr-1Mo-V-Nb Steels*, J-4672, Climax Molybdenum Company of Michigan, Ann Arbor, MI, 1981.

4. G. C. Bodine, C. Chakravarti, C. M. Owens, B. W. Roberts, D. M. Vandergriff, and C. T. Ward, *A Program for the Development of Advanced Ferritic Alloys for LMFBR Structural Application*, ORNL/Sub-4291/1, TR-MCD-015, Oak Ridge National Laboratory, 1977.

5. N. Saunders and A. P. Miodownik, *Calphad (Calculation of Phase Diagrams): A Comprehensive Guide*, Pergamon Materials Series, Volume 1, Elsevier Science Inc., New York, 1998.

6. K. J. Irvine, D. J. Crowe, and F. B. Pickering, "The Physical Metallurgy of 12% Chromium Steels," *J. Iron and Steel Inst.*, vol. 195, pp. 386-405, (1960).

7. J. O. Andersson, "A Thermodynamic Evaluation of the Fe-Cr-C System," *Met. Trans. A*, vol. 19A, pp. 627-636, (1988).

8. E. C. Bain and H. W. Paxton, *Alloying Elements in Steel*, American Society for Metals, 1966.

9. R. W. K. Honeycombe and H. K. D. H. Bhadeshia, *Steels: Microstructure and Properties*, Edward Arnold division of Hodder Headline PLC, 1995.

10. L Béres, W. Irmer, and A. Balogh, "Inconsistency of classification of creep resistant steels in European standard EN 288-3," *Science and Technology of Welding and Joining*, vol. 2, pp. 236-238, (1997).